

Modelling And Simulation of a Batch Reverse Osmosis Process Using Modelica

B Sai Mukesh Reddy¹, Mrugesh Joshi², Seongpil Jeong³, Jaichander Swaminathan^{1*}

¹ICER, Indian Institute of Science Bengaluru, India¹, {saimukesh, jaichander}@iisc.ac.in

²Mechanical Engineering Discipline, IIT Gandhinagar, Gujarat, India², mrugesh.joshi@iitgn.ac.in

³Division of Energy & Environment Technology, KIST 02792, Seoul, Korea³, spjeong@kist.re.kr

Abstract

Batch operation of reverse osmosis (RO) has emerged as a promising strategy for enhancing energy efficiency and reducing fouling in seawater and brackish water desalination applications. This study implements a transient numerical model using Modelica to investigate the behavior of a batch seawater RO (BSWRO) system. The feed solution volume decreases and its salinity increases with time. It is pressurized by pumping product water into the other side of a piston. The model incorporates features such as the feed solution residence time in the inlet and outlet piping and captures the local variation in flux and concentration polarization over the membrane area. The instantaneous power consumption of the high-pressure and circulation pumps is calculated. The ease of adoption of Modelica underscores its utility in simulating complex transient and non-linear phenomena. The developed model can be expanded in the future to answer questions related to optimal control of batch RO systems.

Keywords: Batch Reverse Osmosis, Modelica, mathematical modeling, transient

Nomenclature

Symbol	Name	Units
Q	flowrate	l/h
s	salinity	g/l
t	time	s
P	pressure	Pa
v	velocity	m/s
ΔL	individual membrane discrete element length	m
ρ	density	kg/m ³
f	friction factor	-
A	area	m ²
α	permeability coefficient	m/s.Pa
D_h	hydraulic diameter	m
D_e	diffusivity	m ² /s
k	mass transfer coefficient	m/s
N_{Re}	Reynolds number	-
ν	kinematic viscosity	m ² /s
π	osmotic pressure	Pa
J	mass flux	kg/m ² s
D_i	internal diameter of pipe	m

Δx	individual pipe element length	m
w	specific energy consumption	kWh/m ³
n	Osmotic Pressure coefficient	-

Subscripts

Symbol	Definition
f	feed
r	reject
p	permeate, pipe
cs	cross section
avg	average
in	inlet
out	outlet
m	membrane-feed interface
t	tank
b	bulk
tot	total
atm	atmospheric

Abbreviations

Symbol	Definition
RO	Reverse Osmosis
BRO	Batch Reverse Osmosis
CP	Concentration Polarization
OM	Open- Modelica
PS	Pressure Sensor
ERD	Energy recovery devices
OOP	object-oriented programming
SEC	Specific Energy Consumption
HPP	High Pressure Pump

1 Introduction

The Reverse Osmosis (RO) process, which is widely utilized for desalination, water purification, and wastewater treatment, is commonly operated in continuous flow mode. Batch reverse osmosis (BRO) systems can achieve higher recovery rates with lower energy consumption compared to continuous RO systems. In batch RO, the applied pressure is increased gradually to make-up for the increasing osmotic pressure of the saline brine being treated. As a result, BRO process can approach the thermodynamic energy minimum more closely than continuous processes, enabling significant energy savings (Werber et al., 2017). Batch and hybrid batch/semi-batch configurations are especially suitable for high recovery

desalination where the osmotic pressure of the final brine is significantly higher than that of the feed inlet (Patel et al., 2024). Additionally, batch configurations allow for enhanced process flexibility and can eliminate the need for energy recovery devices. To evaluate the economic feasibility of BRO process and design them optimally, mathematical modelling is employed.

Modeling and simulation of the BRO processes are critical for understanding the complex physical phenomena governing system behavior, such as pressure variation, flow rate and salinity changes, fouling dynamics, and power consumption. The variation of these phenomena locally across the membrane surface are often challenging to observe or measure experimentally, making modeling an essential tool for simulating various operating conditions and studying the behavior of concentration polarization and fouling. Through modeling, these parameters can be examined in greater detail, facilitating better optimization strategies and process designs that may not be achievable through experimental methods alone (Ghernaout, 2017).

While substantial research has focused on modeling continuous RO processes, with studies by Lee et al. (Lee et al., 2010) and Jeong et al. (Jeong et al., 2021) addressing membrane behavior, concentration polarization, and fouling in such systems, modeling of batch RO systems remains limited. Only a few studies (Barello et al., 2015; Kim & Park, 2024; Warsinger et al., 2016; Wei, n.d.), have explored batch processes in detail. However, comprehensive models specific to BRO systems that consider transient conditions, are limited. The need for more detailed models arises due to the unique dynamics of time-dependent concentration polarization and permeate removal, which are not fully captured by existing models.

Modelica, an object-oriented modeling language for complex systems (Fritzson & Engelson, n.d.; Introduction to Object-Oriented Modeling and Simulation with OpenModelica, n.d.; Loeffler et al., 2006), provides an ideal platform for simulating BRO processes. Unlike traditional simulation tools, Modelica enables the creation of reusable components that can be easily adapted to different system configurations, offering better flexibility in modeling BRO systems. Al-Zainati et al. (Al-Zainati et al., 2022) used Modelica for modeling a continuous RO system. Modelica's capabilities in developing dynamic control systems make it particularly useful for optimizing operational parameters such as pressure, flow rate, and recovery ratio, all of which are crucial for efficient BRO operation. Despite these advantages, no studies have yet applied Modelica to model BRO systems. This gives the opportunity to leverage this tool for simulating and controlling BRO processes.

Overall, this work presents the development of a BRO model using Modelica language and Open-Modelica as the tool to simulate key variables such as local pressure, flux, salinity variations and overall permeate production rate over time. By utilizing Modelica's strengths in

reusability, flexibility, and control system modeling, this study proposes a promising approach for advancing the simulation of batch RO processes.

2 Theoretical Background

BRO process which is depicted in **Figure 1** operates by treating a fixed volume of recirculated feedwater until a desired overall recovery is achieved. This is different from a conventional continuous RO process where the desired recovery is achieved in a single pass through the membrane element. The process begins with feed water being filled into the tank, pipes, and membrane element, displacing the final reject brine from the previous cycle. The current model focuses on the dynamics of the system after this point, and hence the local salinity throughout the system is set equal to the feed salinity at $t = 0$.

This feed is circulated from the tank into the membrane element and back into the tank by a circulation pump that works to overcome the frictional losses in the channel and piping. This entire loop is pressurized to overcome the osmotic pressure and drive pure water flux through the membrane. Unlike in continuous RO, where the applied pressure at the inlet to the membrane is maintained at a nearly constant value with time, in BRO, pressure is increased with time to dynamically adjust for the increasing osmotic pressure as the solution gets more concentrated. This dynamic adjustment is the key reason for energy savings which minimizes the unnecessary excess pressure application in conventional continuous RO to achieve the same average flux. Due to these dynamic changes in pressures and concentrations over time, a transient model is needed to study the process in detail.

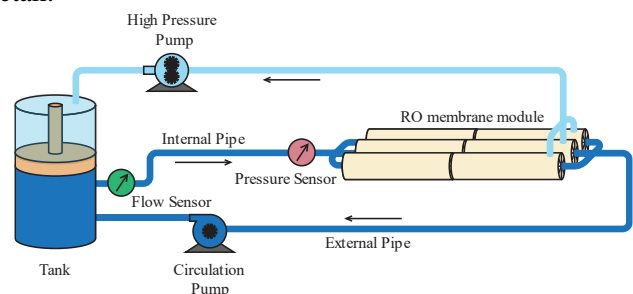


Figure 1 Batch Reverse Osmosis Process

2.1 Modelling of BRO process – Overall flowsheet

Modelling a BRO process involves capturing the dynamic nature of its operation, where feedwater undergoes cyclic pressurization and permeate recovery. One of the critical considerations is the variation in pressure over time, which must match the increasing osmotic pressure as the brine becomes more concentrated. Models must also account for concentration polarization (CP), which affects local flux and energy consumption by reducing effective driving pressure for water transport through the membrane. Energy consuming and energy recovery devices like

pumps and turbines (if any) which are a part of the BRO systems, must be included in the model to estimate net energy consumption accurately.

Modelica's object-oriented programming (OOP) approach offers significant advantages in reducing redundant code and enabling efficient reuse of components. In the modelling of BRO systems, a reusable connector is developed to carry information on pressure, salinity, and flow rate. This connector can be flexibly utilized for the feed, reject, or permeate stream, depending on the specific application. Finite volume models for RO and pipe elements are created and structured to allow extension, facilitating the development of complete RO and pipe network models.

Additionally, separate models for tanks and pumps are designed for integration into the overall process. These individual components are then assembled into a complete flowsheet. This flowsheet serves as a basis for detailed mathematical simulations, for analysing system performance and transient dynamics in BRO processes. The overall architecture to model the BRO systems in Open-Modelica (OM) is given in the **Figure 2**.

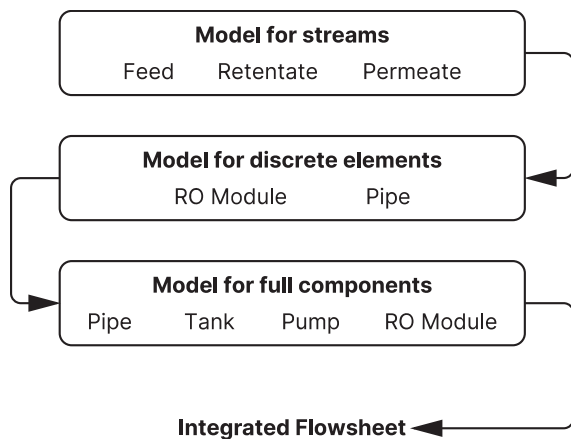


Figure 2 Architecture for BRO system modeling in OM

2.2 Modeling of individual components

2.2.1 Modeling of RO element

In the initial proof-of-concept model developed here, several simplifying assumptions are made such as treating membrane properties like water permeability coefficient (α) and feed density as constant. These assumptions can be relaxed in future work. While the RO process is often assumed to operate under steady-state conditions with negligible pressure losses due to pipe friction, this paper accounts for frictional pressure drop in the pipes and membrane channels. Concentration polarization near the membrane surface is modeled using the film theory to account for solute accumulation near the membrane interface due to water flux from the bulk solution.

The rate of change of local salinity at each feed node is calculated using Eq. (1). Since feed density variations are assumed to be small, Eq. (2) governs the overall solution mass balance at each node, accounting for water transport

through the membrane as product. Local water flux is calculated using equation 1, which depends on pressure and osmotic differences across the membrane. Osmotic pressure of the feed is calculated using the equation 11, while the local concentration polarization is given by Eq. 10. The channel pressure drop is accounted for using the Haigen Poiseuille equation 3.

$$\frac{ds}{dt} = Q_f \cdot s_f - Q_r \cdot s_r - Q_p \cdot s_p \quad (1)$$

$$Q_f = Q_r + Q_p \quad (2)$$

$$\frac{P_f - P_r}{\Delta L} = \frac{2\rho v_{avg}^2 f}{D_h} \quad (3)$$

$$v_f = \frac{Q_f}{A_{cs}} \quad (4)$$

$$v_{avg} = \frac{v_f + v_r}{2} \quad (5)$$

$$Re = \frac{D_h v_{avg}}{\nu} \quad (6)$$

$$k = 2.53 \frac{D_e}{D_h} \cdot \left(16Re^2 + \frac{0.4892}{Re^{0.2964}} \right) \quad (7)$$

$$f = \frac{16}{Re} + \frac{0.4892}{Re^{0.036}} \quad (8)$$

$$J = \alpha(P_{avg} - \pi_m) \quad (9)$$

$$s_m = s \cdot e^{\frac{J}{k}} \quad (10)$$

$$\pi_m = \pi_0 s_m^n \quad (11)$$

2.2.2 Modeling of Tank

The tank is assumed to be well-mixed, which ensures that the salinity within the tank remains uniform at any given time. This assumption eliminates the need to model spatial variations in the tank, which may be considered in later detailed analyses. The governing equations 12,13 represent volume and salinity balances in the tank. These equations incorporate time-dependent dynamics of volume and salinity based on inflow and outflow of the tank which are readily available using the connectors.

$$\frac{dV}{dt} = Q_{t,in} - Q_{t,out} \quad (12)$$

$$\frac{d(V \cdot s)}{dt} = s_{t,in} \cdot Q_{t,in} - s_{t,out} \cdot Q_{t,out} \quad (13)$$

2.2.3 Modeling of Pipe element

Modeling a pipe in Modelica to account for salinity and pressure variations involves representing mass and momentum balances along its length. The salinity changes are governed by equation 14, where flow rates (Q) and salinity (s) are measured at both inlet and outlet. Pressure drop is modeled using the Darcy-Weisbach equation 15, with the friction factor as f_p . The model assumes steady flow in a cylindrical pipe with constant fluid properties and negligible heat transfer. In Modelica, connectors handle pressure, flow rate, and salinity inputs and outputs, enabling integration with other system components. Mass and momentum balances are implemented with equations

capturing salinity transport and pressure loss, while spatial discretization ensures accurate simulation of flow characteristics along the length of the pipe.

$$V \frac{ds}{dt} = s_{p,in} \cdot Q_{p,in} - s_{p,out} \cdot Q_{p,out} \quad (14)$$

$$\frac{P_{p,in} - P_{p,out}}{\Delta x} = \frac{\rho v_{avg}^2 f_p}{2 \cdot D_i} \quad (15)$$

2.3 Flowsheet Simulation in Open Modelica

The individual models explained in section 2.2 for the tank, pipe, and RO modules were systematically integrated to create a complete flowsheet representation of the BRO process as shown in **Figure 3**. Each module is designed to operate independently, with connectors enabling data transfer. By combining these modular components, the flowsheet can capture the dynamic interactions between the tank, pipes, and the RO module. The flowsheet integrates these models to represent the physical experimental setup, providing a comprehensive framework for simulating the process.

In the overall flowsheet, initial conditions are set for salinity throughout the system. Initial values are also set for variables involved in non-linear equations to ensure numerical stability and solution convergence. These initial values allow the system to reach the desired operational state efficiently, replicating realistic startup and steady-state conditions. Using OM, the interconnected components facilitate the study of the BRO process under various scenarios, enabling detailed analysis of system performance, such as energy consumption, recovery efficiency, and pressure profiles. The modular structure of the flowsheet also allows for easy scalability and customization, supporting future extensions or modifications, such as adding energy recovery devices or advanced control schemes.

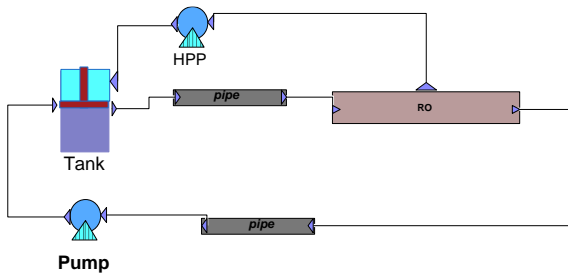


Figure 3 Flowsheet simulation of BRO process in Open Modelica

2.4 Specific Energy Consumption

The specific energy consumption (SEC) is a critical parameter in evaluating the efficiency of a BRO process. It is calculated based on the total mass of permeate produced and the energy consumption of the pumps over the operating time. For each pump the high-pressure pump and the recirculation pump, the energy consumption at each time step is determined as the function of the volumetric flow rate, the pressure differential, and the pump efficiency.

The equation 16 is used to calculate SEC in this study. Note that the actual SEC may be higher when factors such as permeate back-flux and pump energy usage during the cycle reset are considered.

$$w = \frac{W_{tot}}{Q_p} \quad (16)$$

$$W_{HPP} = Q_p \cdot (P_{t,out} - P_{atm}) / \eta_{HPP} \quad (17)$$

$$W_{CP} = Q_{t,in} (P_{t,out} - P_{t,in}) / \eta_{CP} \quad (18)$$

$$W_{tot} = W_{HPP} + W_{CP} \quad (19)$$

3 Results and Discussions

The critical parameters and constants for the membrane are given in the **Table 1**. The simulations were conducted using Open-Modelica software version 1.23.0 on a computing system equipped with a 13th Gen Intel(R) Core (TM) i9-13900K processor (3.00 GHz), 64 GB RAM, and a 64-bit operating system. All transient simulations were carried out over a one-hour period, equivalent to 3600 seconds of runtime with a 60 second time step, to capture the system's dynamic behaviour under operational conditions.

Table 1 Parameters

Symbol	Value	Units	Description
RO membrane module			
W	20	m	Width of the channel
L	1	m	Length of the channel
H	7e-4	m	Height of the channel
N	50	-	Number of finite elements discretized
α	2.7e-7	m/(s·Pa)	Permeability coefficient
D_e	1.5e-9	m ² /s	Diffusivity coefficient
D_h	8.2e-4	m	Hydraulic diameter
A_{mem}	40	m ²	Available area for the membrane
A_{cs}	0.014	m ²	Cross-sectional area of the channel
J_{avg}	15	kg/(m ³ ·hr)	Average permeate flux
RR	0.5	-	Recovery Ratio
Tank			
V	1.2	m ³	Volume of the tank
$Area$	0.4	m ²	Area of the tank
Pipe			
D_i	0.0762	m	Internal Diameter of the pipe
L	0.5	m	Length of the pipe
Pumps			
η_{CP}	0.9	-	Efficiency of the circulation pump
η_{HPP}	0.9	-	Efficiency of the HPP

3.1 Transient Analysis of Salinity and Flux Variation Along the Membrane Length

Figure 4 illustrates how local salinity changes across the length of a 1-meter membrane length over time. The membrane is discretized into 50 equal sections of 0.02-meter length each. The local salinity variation along the membrane length is plotted at different time-steps during the process. The first line corresponds to $t = 1$ min, the second at $t = 11$ min, and the final line at $t = 60$ min (1 hour).

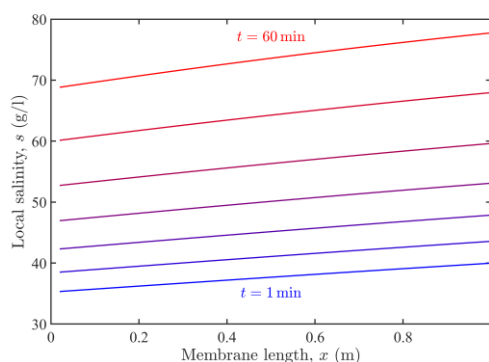


Figure 4 Local salinity profile along the length of the membrane for increasing time

Initially, all the water in the RO module is at 35 g/l salinity. But as the time progresses, salinity in RO increases due to permeate production. At the same time, feed entering the RO module is less saline compared to the local brine. Hence, at the start of the membrane, salinity is lower compared to end of the membrane where gradually more permeate is recovered along the flow. As time progresses, tank gets much more saline as less volume of low salinity water mixes with same amount of brine. Therefore, feed entering the module gets even more saline, resulting in steeper increase in inlet salinity with time. This makes salinity gradient along the membrane more pronounced with time. This effect is captured in Figure 4.

3.2 Transient Analysis of Flux Variation Along the Membrane Length

Figure 5 illustrates how the flux changes along the membrane length at each single node of the membrane element. The spatial variance in flux increases with time. This can be explained by effect of salinity as shown in Figure 4 as well as pressure drop along the module length. At any given time, pressure at inlet is higher compared to pressure at the outlet. Therefore, first term in driving force ($P - \pi_m$) is less at outlet compared to inlet. Also, as explained in Figure 4, salinity at inlet is lower compared to salinity at the outlet. Hence, the second term in the driving force is more at outlet compared to inlet. These both effects simultaneously make flux at outlet less compared to inlet. Specifically, as salinity gradient along the membrane length increases with increase in time, flux variance also increases with time. This effect is captured by the model and shown in **Figure 5**.

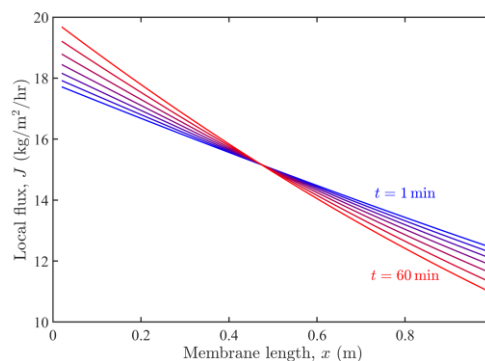


Figure 5 Local permeate flux profile along the length of the membrane for increasing time

3.3 Pressure Changes in the Tank

Figure 6 shows how pressure increases with time in batch RO operation when a constant flux is maintained. This is due to increase in average feed salinity as more permeate is recovered. This increased salinity results in increase in osmotic pressure of the tank and consequently of the feed. Therefore, pressure is further increased to maintain a constant permeate flux. As salinity increases slowly at first when the volume of the tank is larger, the same trend is observed for pressure in **Figure 4**, where the pressure increases more rapidly at later times.

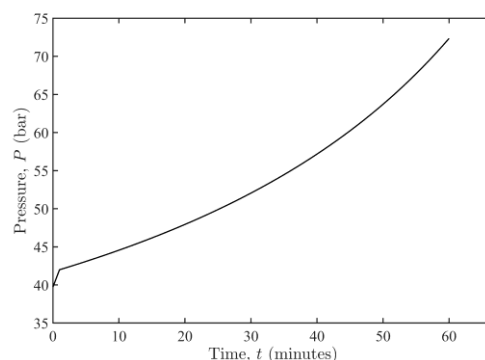


Figure 6 Pressure changes with time for a fixed average flux

3.4 Energy consumption

Figure 7 represents the relationship between the specific energy consumption (w) and the average permeate flux (J_{avg}). The x-axis shows the set or fixed average permeate flux, while the y-axis indicates the specific energy consumption of the two pumps used in the process, which operate under varying pressure conditions in the tank.

As the average permeate flux increases, the specific energy consumption rises significantly. This trend occurs because higher permeate flux requires greater pressure differences across the membrane, leading to increased energy demands for the pumps. At lower flux values, the energy consumption is relatively low due to smaller pressure requirements. However, as the flux increases, the pressure requirements rise non-linearly, causing a steep increase in specific energy consumption.

This graph highlights the trade-off between achieving higher permeate flux and maintaining energy efficiency. The results emphasize the importance of optimizing operational parameters to balance water production and energy consumption in reverse osmosis systems.

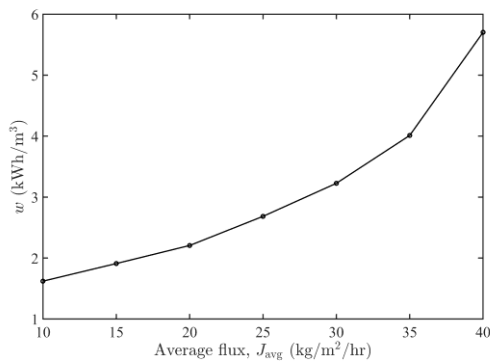


Figure 7 Average Permeate flux vs SEC

4 Conclusion

This study demonstrates the effectiveness of using an OOP approach in Open-Modelica to model and analyse the transient dynamics of BRO systems. By integrating modular components such as the membrane, tank, and pipe models into a comprehensive flowsheet, the system's behaviour under varying conditions was successfully simulated. The transient simulations revealed key insights into salinity and flux variation along the membrane length and variation in specific energy consumption rate of the system with time.

The relationship between average permeate flux and specific energy consumption underscores the need to optimize operating conditions to achieve a balance between performance and energy efficiency. The modelling framework helps explain the dynamic behaviour of BRO systems and paves the way for further optimization of the BRO process.

Acknowledgements

This collaborative work between Indian Institute of Science Bengaluru and Korean Institute of Science and Technology has been supported and funded by Department of Science and Technology, Government of India, (Project no. INT/Korea/P-690) and Indian Institute of Science Bengaluru.

References

- Al-Zainati, N., Subbiah, S., Yadav, S., Altaee, A., Bartocci, P., Ibrar, I., Zhou, J., Samal, A. K., & Fantozzi, F. (2022). Experimental and theoretical work on reverse osmosis - Dual stage pressure retarded osmosis hybrid system. *Desalination*, 543. <https://doi.org/10.1016/j.desal.2022.116099>
- Barello, M., Manca, D., Patel, R., & Mujtaba, I. M. (2015). Operation and modeling of RO desalination process in batch mode. *Computers and Chemical Engineering*, 83, 139–156. <https://doi.org/10.1016/j.compchemeng.2015.05.022>
- Fritzson, P., & Engelson, V. (n.d.). *Modelica-A Unified Object-Oriented Language for System Modeling and Simulation*.
- Ghernaout, D. (2017). Reverse Osmosis Process Membranes Modeling-A Historical Overview. *Journal of Civil, Construction and Environmental Engineering*, 2(4), 112–122. <https://doi.org/10.11648/j.jccee.20170204.12>
- Introduction to Object-Oriented Modeling and Simulation with OpenModelica*. (n.d.).
- Jeong, K., Son, M., Yoon, N., Park, S., Shim, J., Kim, J., Lim, J. L., & Cho, K. H. (2021). Modeling and evaluating performance of full-scale reverse osmosis system in industrial water treatment plant. *Desalination*, 518. <https://doi.org/10.1016/j.desal.2021.115289>
- Kim, G. Y., & Park, K. (2024). Application of batch reverse osmosis as an appropriate technology for inland desalination: Design, modeling, and operating strategies. *Desalination*, 592. <https://doi.org/10.1016/j.desal.2024.118185>
- Lee, S., Boo, C., Elimelech, M., & Hong, S. (2010). Comparison of fouling behavior in forward osmosis (FO) and reverse osmosis (RO). *Journal of Membrane Science*, 365(1–2), 34–39. <https://doi.org/10.1016/j.memsci.2010.08.036>
- Loeffler, M., Huhn, M., Richter, C., & Kossel, R. (2006). *The Modelica Association Modelica* (Vol. 4).
- Patel, D., Ankoliya, D., Raninga, M., Mudgal, A., Patel, V., Patel, J., Mudgal, V., & Choksi, H. (2024). Batch Reverse Osmosis: Evolution from the Concept to the Technology. In A. Mudgal, P. Davies, M. Kennedy, G. Zaragoza, & K. Park (Eds.), *Advances in Water Treatment and Management* (pp. 175–200). Springer Nature Singapore.
- Warsinger, D. M., Tow, E. W., Nayar, K. G., Maswadeh, L. A., & Lienhard V, J. H. (2016). Energy efficiency of batch and semi-batch (CCRO) reverse osmosis desalination. *Water Research*, 106, 272–282. <https://doi.org/10.1016/j.watres.2016.09.029>
- Wei, Q. J. (n.d.). *BATCH REVERSE OSMOSIS: EXPERIMENTAL RESULTS, MODEL VALIDATION, AND DESIGN IMPLICATIONS*.
- Werber, J. R., Deshmukh, A., & Elimelech, M. (2017). Can batch or semi-batch processes save energy in reverse-osmosis desalination? *Desalination*, 402, 109–122. <https://doi.org/10.1016/j.desal.2016.09.028>